RBCM - J. of the Braz. Soc. Mechanical Sciences ISSN 0100-7386
Vol. XX - No 4 - 1998 - pp. 576-586 Prined in Brazil

On the Effect Of Temperature in Non-Linear Dynamics of an Elasto-Plastic Oscillator with Isotropic Hardening

Marcelo Amorim Savi
Instituto Militar de Engenharia
Departamento de Engenharia Mecânica e de Materiais
22290-270 Rio de Janeiro, RJ. Brazil
savi@ime.eb.br

Pedro Manuel Calas Lopes Pacheco
CEFET-RJ
Departamento de Engenharia Mecânica
20.271.110 Rio de Janeiro, RJ. Brazil
calas@cefet-rj.br

Abstract

This contribution presents a dynamical analysis of an elasto-plastic oscillator where the thermomechanical coupling is considered. A constitutive model, used to describe the restitution force of the oscillator, is presented. Isotropic hardening is considered. Operator split technique is used to develop a numerical procedure. An integrator scheme associated with return mapping algorithm is used to solve the equations of motion. Numerical simulations show that the effect of thermomechanical coupling may produce an unstable response.
Key Words: *Non-linear Dynamics, Elasto-plasticity, Modeling and Simulation.*

Introduction

The elasto-plastic behavior describes the deformation mechanisms of most metals and alloys at room temperature. The theories of elasticity and plasticity are both based on experimental studies of stress-strain relations in polycrystalline aggregate under simple load conditions. Hardening effect represents the way of how plastic strains modify the yield surface. It is an usually situation and has many different ways to occur, depending specifically on the material considered. There are many idealized models to describe hardening effect. A great number of situations involving cyclic loadings can be properly represented by isotropic hardening which corresponds to an uniform expansion of the yield surface (Lemaitre and Chaboche, 1990).

The hypothesis of isothermal process is usually adopted in dynamical analysis of metallic structures. For metallic components submitted to plastic cyclic loadings, however, part of plastic work is transformed into heat, resulting in a temperature rise which can affect substantially the mechanical behavior.

A feedback phenomenon can be promoted by the thermomechanical coupling. The heat generated by the mechanical process causes the increase of temperature which promotes the mechanical strength decrease. As a consequence, the amplitude of plastic strains tends to growth which causes a greater temperature rise and so on. This behavior only happens for some special conditions where an unstable behavior is expected.

This contribution reports to a dynamic analysis of an elasto-plastic oscillator where the thermomechanical coupling is considered. The restitution force of the oscillator is considered by a constitutive model with internal variables where the coupling effects are introduced. Isotropic hardening is considered. A numerical method is developed using an implicit integration scheme associated with the return mapping algorithm. Operator split technique is used. Some numerical simulations are presented for forced vibrations and show that the isothermal hypothesis is inadequate to describe some situations where cyclic inelastic deformations are involved.

Anisothermal Elasto-Plastic Model

A constitutive model to describe the elasto-plastic behavior is considered assuming an additive decomposition, *i.e.*, the total displacement x may be splitted into an elastic part, x^e, and a plastic part, x^p. Including temperature effects in the model, the force-displacement relation is given by the following equation:

$$p = K\left[(x - x^p) - \alpha_t L(\theta - \theta_0)\right] , \tag{1}$$

where K is a stiffness parameter, α_t the thermal expansion coefficient, L is the total length, θ the absolute temperature and θ_0 the initial temperature of the elasto-plastic element.

The isotropic hardening is described by introducing an internal variable, α, referred to as *internal hardening variable*. A simple evolution equation to this variable considers that the hardening is linear in the amount of plastic flow, $\dot{x}^p$, and independent of the sign of this flow, $sign(\dot{x}^p)$ (Simo, 1994). This may be expressed by,

$$\dot{\alpha} = \left|\dot{x}^p\right| . \tag{2}$$

Experimental observations establish that the plastic displacement has the following evolution equation (Simo, 1994):

$$\dot{x}^p = \dot{\gamma}\, L sign(p) , \tag{3}$$

where $\dot{\gamma}$ represents the rate at which plastic deformation take place and is called plasticity multiplier.

The elastic region is defined by the plasticity function (Simo and Miehe, 1992):

$$h(p,\alpha,\theta) = \left|p\right| - y(\alpha,\theta) , \tag{4}$$

where

$$y(\alpha,\theta) = S\left[y_0 + (y_\infty - y_0)(1 - e^{-\delta\frac{\alpha}{L}}) + h_\alpha \frac{\alpha}{L} \right]\left[1 - h_\theta(\theta - \theta_{ref})\right] , \tag{5}$$

and y_0 , y_∞ , h_α , h_θ and δ are material parameters, θ_{ref} is a reference temperature associated with the initial temperature, θ_0, and S the cross section area of the elasto-plastic element of the oscillator. The form of this hardening function shows that the increase of internal hardening variable causes elastic domain expansion, while the increase of temperature causes the shrinkage of this domain.

The irreversible nature of plastic flow is represented by means of the *Kuhn-Tucker conditions* (Luenberger, 1973). Another constraint must be satisfied when $h(p,\alpha,\theta)=0$. It is referred as *consistency condition* (Simo, 1994). These conditions are presented as follows:

$$\begin{aligned} &\dot{\gamma} \geq 0 \\ &\dot{\gamma}\, h(p,\alpha,\theta) = 0 \\ &\dot{\gamma}\, \dot{h}(p,\alpha,\theta) = 0 \quad \text{if} \quad h(p,\alpha,\theta) = 0 \end{aligned} \tag{6}$$

Disregarding the source term, the energy equation can be written as (Pacheco, 1994):

$$\rho c_e \dot{\theta} = \frac{\chi\, p\, \dot{x}^p}{L\, S} - \frac{h_c\, S_p}{S}(\theta - \theta_0) , \tag{7}$$

where ρ is the density, c_e the specific heat, h_c the convection parameter from the traditional hypothesis of fins and S_p the cross section perimeter of the elasto-plastic element of the oscillator. The first term on the right side of the energy equation is called the internal thermomechanical coupling and is associated with the internal dissipation of the mechanical process. The empirical parameter χ is called heat conversion factor and indicates the amount of plastic power that is converted into heat (Pacheco, 1994).

Elasto-Plastic Oscillator

Considering a single degree of freedom oscillator with mass *m* and an external linear viscous dissipation parameter *c*, the balance of linear momentum is given by the equation,

$$m\ddot{x}+c\dot{x}+p(x,x^p,\alpha,\theta)=f(t) \ , \tag{8}$$

where $p(x,x^p,\alpha,\theta)$ is the elasto-plastic restitution force of the oscillator and f(t) is an external force.

Defining the variables $v=\dot{x}$ and $\omega_0^2=K/m$, the following non-dimensional variables are used,

$$\tau=\omega_0 t \ ; \quad \Omega=\omega/\omega_0 \ ; \quad P=p/(E\,S); \quad F=f/(E\,S) \ ;$$

$$X=x/L \ ; \ X^p=x^p/L; \ V=v/(\omega_0 L); \ A=\alpha/L; \quad T=\theta/\theta_{ref} \ ; \tag{9}$$

where E is a material parameter. Considering $\mathbf{X}=(X,V,X^p,A,T)$, the equations of motion are like $\dot{\mathbf{X}}=\mathrm{F}(\mathbf{X},\tau),\mathbf{X}\in\Re^5$, associated with complementary conditions (6). Hence, assuming a periodic excitation $F(\tau)=F_0\sin(\Omega\tau)$, it is possible to write the following equations of motion:

$$\dot{X}=V$$

$$\dot{V}=F_0\sin(\Omega t)-c_0V-(X-X^p)+\Lambda_T(T-1)$$

$$\dot{X}^p=\dot{\gamma}\,sign(P)$$

$$\dot{A}=\dot{\gamma}$$

$$\dot{T}=\varphi P\dot{X}^p-\xi(T-1)$$

$$h(P,A,T)=|P|-Y(A,T) \tag{10}$$

where

$$c_0=\frac{c}{m\,\omega_0}$$

$$\Lambda_T=\alpha_t\,\theta_{ref}$$

$$\varphi = \frac{\chi \, \mathrm{E}}{\rho \, \mathrm{c_e} \, \theta_{\mathrm{ref}}}$$

$$\xi = \frac{\mathrm{h_c S_p}}{\rho \, \mathrm{c_e} \, \omega_0 \, \mathrm{S}}$$

and $$Y(A,T) = \frac{y(\alpha,\theta)}{E\,\mathrm{S}} = \left[Y_0 + (Y_\infty - Y_0)(1 - e^{-\delta A}) + H_A A\right]\left[1 - H_T (T-1)\right] \tag{11}$$

with $$Y_0 = \frac{y_0}{E} \quad ; \quad Y_\infty = \frac{y_\infty}{E} \quad ; \quad H_A = \frac{h_\alpha}{E} \quad ; \quad H_T = h_\theta \, \theta_{\mathrm{ref}}$$

Numerical Procedute

The numerical solution procedure here proposed uses the operator split technique (Chorin et al., 1978; Ortiz, Pinsky and Taylor, 1983; Marchuk, 1975) to make the partition of the space of variables in two parts. One part is the phase plane and includes the variables (*X,V*) and the other one is the internal variables and temperature space and includes (X^p,*A,T*). With this split, it is possible to develop a solution procedure by considering an iterative process where each part is treated separately.

The time integration of equations of motion on phase plane can be done by any integration scheme, since the variables X^p, *A* and *T* are considered as known parameters. As a first trial, an elastic predictor step is assumed, where the value of X^p, *A* and *T* cannot vary from the previous time instant. The next step of solution procedure consists on evaluating the feasibility of the trial state. Hence, the *return mapping algorithm* is considered (Simo and Taylor, 1985). Then it is necessary to return to phase plane equations and recalculate the pair (*X,V*) using the new values of the parameters X^p, *A* and *T*. This procedure must be repeated until it converges. This situation occurs when the difference between the actual and trial state reaches a prescribed tolerance.

Return Mapping Algorithm

At this point, a trial state (X_{n+1}, V_{n+1}) is known. This is considered as an input for the return mapping algorithm. A trial state is defined by considering an elastic predictor step, which is written as follows:

$$P_{n+1}^{trial} = (X_{n+1} - X_n^p) - \Lambda_T (T_n - 1) \tag{12}$$

$$(X_{n+1}^p)^{trial} = X_n^p \tag{13}$$

$$A_{n+1}^{trial} = A_n \tag{14}$$

$$T_{n+1}^{trial} = T_n \tag{15}$$

$$h_{n+1}^{trial} = \left| P_{n+1}^{trial} \right| - Y(A_{n+1}^{trial}, T_{n+1}^{trial}) \tag{16}$$

If $h_{n+1}^{trial} \leq 0$, it means that the state is on the elastic domain and the trial state is the actual one. Otherwise, if $h_{n+1}^{trial} > 0$, we are outside the elastic domain and a plastic step must be considered. This step is associated with the determination of the increment of plasticity multiplier ($\Delta\gamma$) on the time instant t_{n+1}, when the plasticity function $h(p,\alpha,\theta)$ must vanish. Using an implicit Euler algorithm to discretize the evolution equations (1-3,7), the plastic step can be written as follows:

$$P_{n+1} = P_{n+1}^{trial} - sign(P_{n+1}^{trial})(1 + \Lambda_T \varphi P_{n+1}^{trial})\Delta\gamma + \Lambda_T \xi (T_{n+1}^{trial} - 1)\Delta\tau \tag{17}$$

$$X_{n+1}^{p} = (X_{n+1}^{p})^{trial} + sign(P_{n+1}^{trial})\Delta\gamma \tag{18}$$

$$A_{n+1} = A_{n+1}^{trial} + \Delta\gamma \tag{19}$$

$$T_{n+1} = T_{n+1}^{trial} + \varphi \left| P_{n+1}^{trial} \right| \Delta\gamma - \xi (T_{n+1}^{trial} - 1)\Delta\tau \tag{20}$$

$$\Delta\gamma = \frac{h_{n+1}^{trial} - \left[M_T - \Lambda_T sign(P_{n+1}^{trial}) \right] \xi (T_{n+1}^{trial} - 1)\Delta\tau}{1 + \Lambda_T \varphi P_{n+1}^{trial} + M_A - M_T \varphi \left| P_{n+1}^{trial} \right|} \quad , \tag{21}$$

where

$$M_A = \left[1 - H_T (T_{n+1}^{trial} - 1) \right] (Y_\infty - Y_0) \delta e^{-\delta A_{n+1}^{trial}} + H_A \Big] \tag{22}$$

$$M_T = H_T \left[Y_0 + (Y_\infty - Y_0)(1 - e^{-\delta A_{n+1}^{trial}}) + H_A A_{n+1}^{trial} \right] \tag{23}$$

A recursive procedure is used to obtain the increment of plasticity multiplier. This process is repeated until this increment reaches a prescribed tolerance to guarantee the convergence to the yield surface. In spite of the strong non-linearities introduced by the temperature, the proposed return mapping algorithm treats the coupled mechanical and thermal equations simultaneously, which permits the use of relatively large time steps.

Numerical Simulations

This section presents some numerical simulations on the behavior of the elasto-plastic oscillator, using the proposed procedure. Forced vibrations are considered. All simulations use the parameters presented on Table 1 (Simo and Miehe, 1992). Time steps less than $\Delta\tau = 2\pi / 800\Omega$ presents a good convergence.

Table 1: Parameters of the Oscillator.

Y_0	2.143 x 10^{-3}
Y_∞	3.405 x 10^{-3}
H_A	6.152 x 10^{-4}
H_T	6.826 x 10^{-6}
χ	0.90
Λ_T	2.930 x10^{-3}
δ	16.93
c_0	2000
φ	1.800 x 10^{2}
ξ	1.098 x 10^{-6}

A feedback phenomenon can be observed for some special conditions where an unstable behavior is expected. The thermomechanical coupling causes an increase of temperature which promotes mechanical strength decrease. As a consequence, the amplitude of plastic strains tends to growth which causes a greater temperature rise and so on. It is important to identify these conditions because wrong predictions can be obtained and unexpected failures may occur, if the thermomechanical effect is not included in the model.

Hence, we are interested to obtain the regions where some qualitatively changes on dynamical system behavior occur as a consequence of parameter variations. That is, we are looking for possible bifurcations on the dynamical behavior of the oscillator.

A bifurcation analysis of the problem is now in focus. The variation of two different parameters are important to be considered: Driving force amplitude, F_0, and frequency, Ω. Bifurcation diagram represents the stroboscopically sampled of some variable under the slow quasi-static increase of the parameter in question (F_0 or Ω).

Figure 1 presents the bifurcation diagram showing the plastic displacement under the variation of driving force amplitude. Two different frequencies are considered: $\Omega = 0.1$ and $\Omega = 0.6$. The variables are sampled on 1/4 of the period for the last 200 cycles of a 1000 cycles simulation. A driving force amplitude which causes a stable response is associated with only one point on the diagram. On the other hand, an amplitude associated with many points, represents an unstable response.

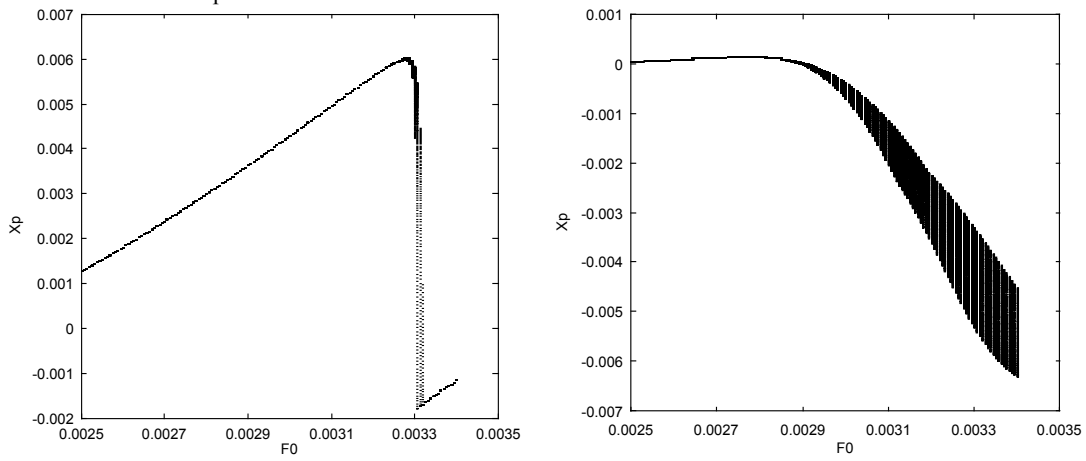

(a) **(b)**

Figure 1: Bifurcation diagram showing the plastic displacement under the variation of the driving force amplitude for (a) $\Omega = 0.1$ and (b) $\Omega = 0.6$.

Figure 2 presents the bifurcation diagram showing the plastic displacement under the variation of driving force frequency. Two different amplitudes are considered: $F_0 = 3.1e-3$ and $F_0 = 3.3e-3$. Again, the variables are sampled on 1/4 of the period for the last 200 cycles of a 1000 cycles simulation. Frequency values associated with only

one point is associated with stable responses while many points are associated with frequency values which presents unstable responses.

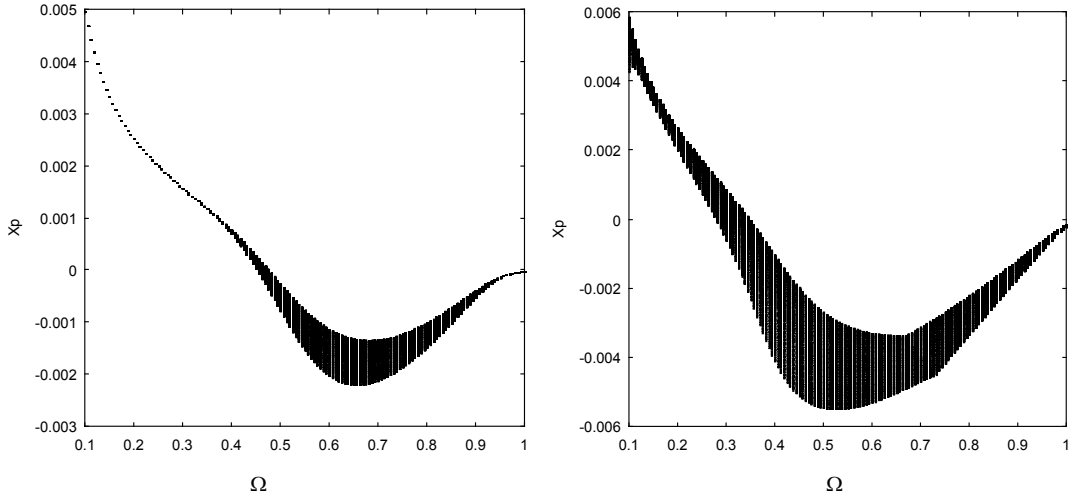

Figure 2: Bifurcation diagram showing the plastic displacement under the variation of the driving force frequency for (a) $F_0 = 3.1e-3$ **and (b)** $F_0 = 3.3e-3$**.**

Now, some particular values of parameters F_0 and Ω are considered. First, consider $F_0 = 3.1e-3$. For this amplitude, $\Omega = 0.1$ corresponds to a stable response while $\Omega = 0.6$ is associated with an unstable behavior. This agrees with the behavior shown in Figure 1-2. Figure 3 shows the plastic displacement time history. Figure 3a shows the response for $\Omega = 0.1$ while Figure 3b shows the response for $\Omega = 0.6$. Figure 4 shows the plastic displacement time history for $F_0 = 3.3e-3$ and the frequencies $\Omega = 0.1$ and $\Omega = 0.6$. Now, both situations present unstable responses, as indicated by Figure 1-2.

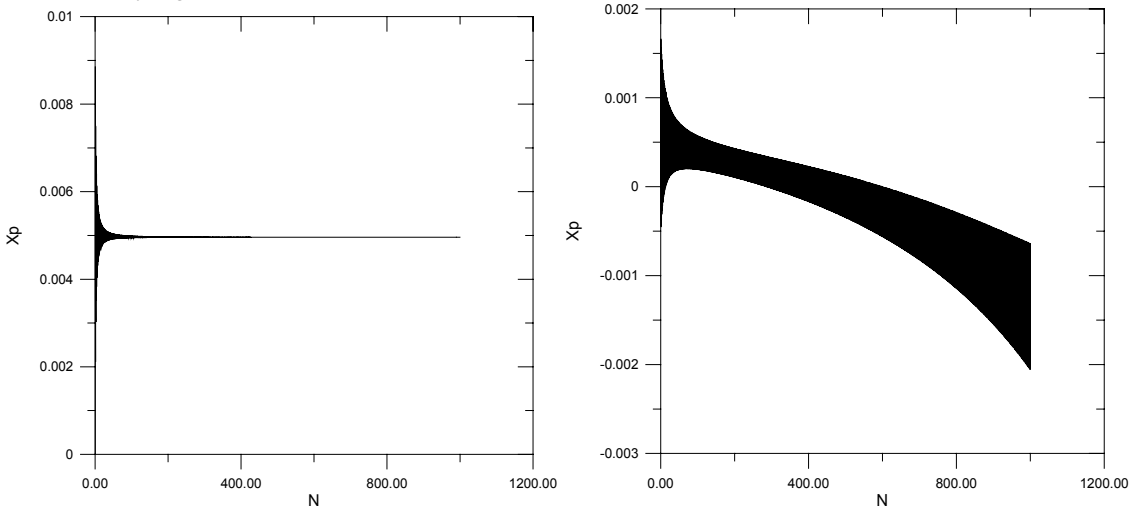

Figure 3: Plastic displacement time history. (a) $F_0 = 3.1e-3$ **and** $\Omega = 0.1$ **;**
(b) $F_0 = 3.1e-3$ **and** $\Omega = 0.6$**.**

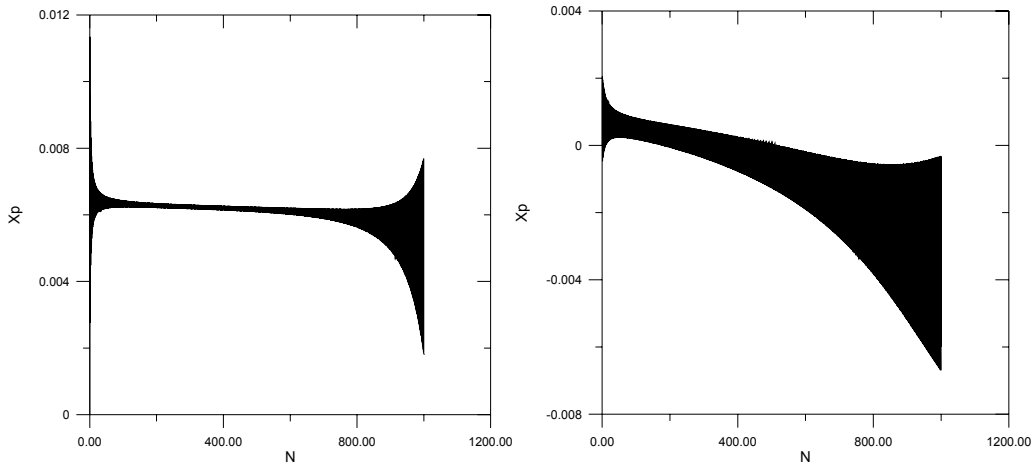

(a) **(b)**

Figure 4: Plastic displacement time history. (a) F_0 = 3.3e-3 and Ω = 0.1; (b) F_0 = 3.3e-3 and Ω = 0.6.

Figure 5 shows temperature, T, and yield function, Y, evolution for different pairs (F_0 , Ω). For the situations where an unstable response is present, anisothermal model predicts a continuous increase in temperature values which causes a decrease in the values of yield function. On the other hand, when a stable response is observed, the temperature and the yield function remains constant, after a short transient.

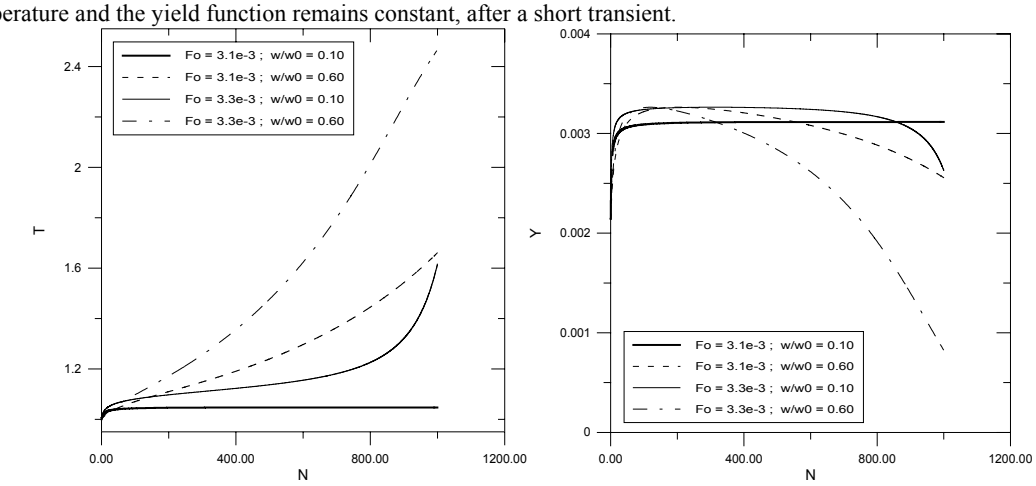

(a) **(b)**

Figure 5: (a) Temperature evolution; (b) Yield function evolution.

Let us consider a situation where an unstable behavior is expected, say F_0 = 3.3e-3 and Ω = 0.1. Figure 6 presents the time history of the other variables of the problem, that is, total displacement, velocity, internal hardening variable and elasto-plastic restitution force. The internal hardening variable, A, evolution presents three distinct regions (Figure 6c). On the initial region, the variable increases quickly. Then a second region is reached, and a smooth increase occurs. The third region presents a high rate growth. This last region is associated with unstable response. Similar behavior is presented by the temperature (Figure 5a). Looking for the other variables (Figure 6a,b,d), it is possible to identify the last region, where the amplitudes begin to vary considerably. Total displacement and velocity tends to increase (Figure 6a,b), while the restitution force tends to decrease (Figure 6d). It is also possible to see that the average values do not vary in a significantly way.

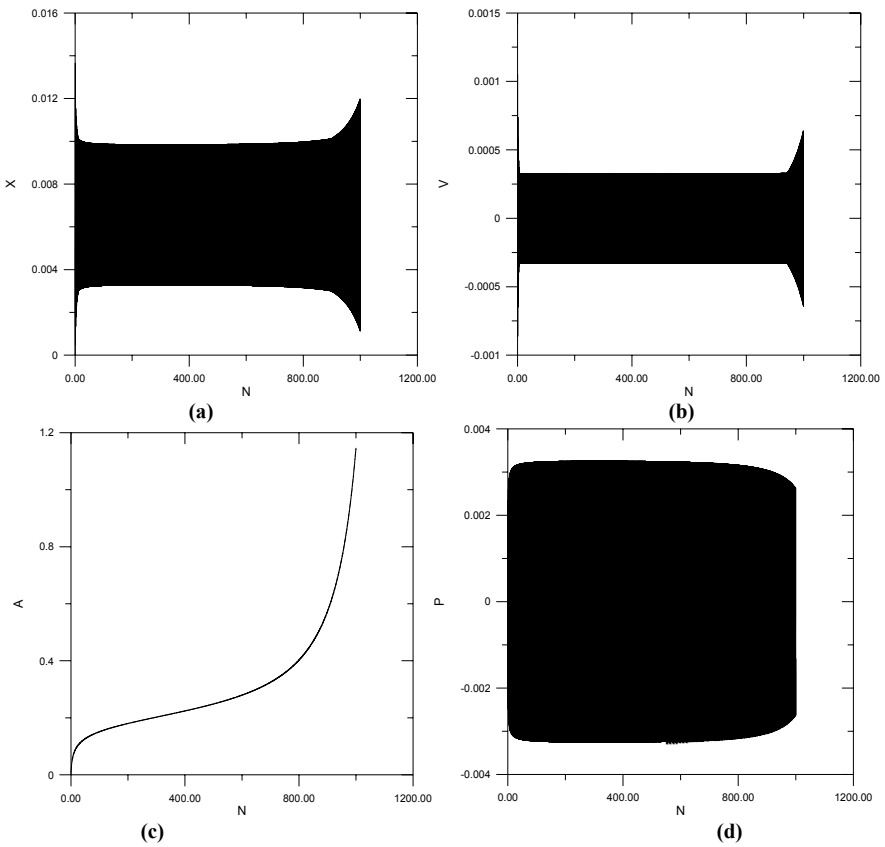

Figure 6: (a) Total displacement evolution ; (b) Velocity evolution ; (c) Internal hardening variable evolution ; (d) Elasto-plastic restitution force evolution.

In the forthcoming analysis, some examples are considered to establish a comparison between isothermal and anisothermal models. Figure 7 presents the total and plastic displacement evolution, predicted by the isothermal model, when F_0 = 3.3e-3 and Ω = 0.1. This Figure permits to see that the isothermal model presents a stable response while the anisothermal model presents an unstable one, as shown in Figure 4a.

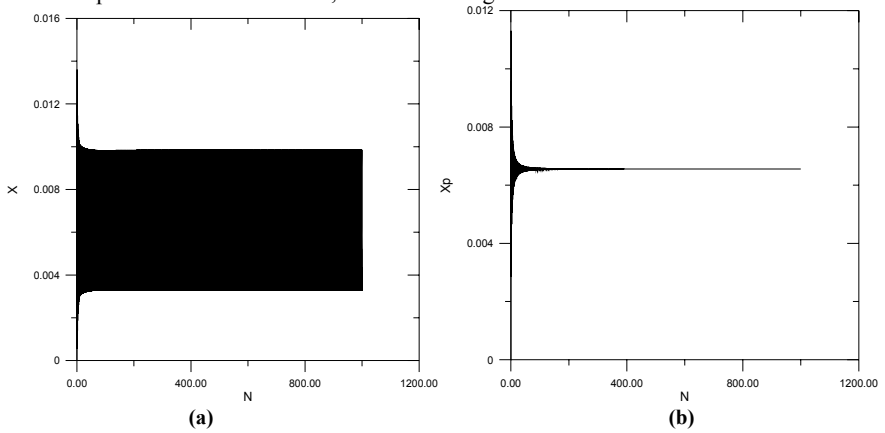

Figure 7: (a) Total displacement ; (b) Plastic displacement evolution for the isothermal model.

Figure 8 shows the evolution of the internal hardening variable and the yield function for the two models. The unstable response observed in the anisothermal model can be associated to an increasing evolution of internal hardening variable (Figure 8a) and to a softening behavior of the yield function (Figure 8b). On the other hand, the stable response observed in the isothermal model is associated to a constant temperature causing a monotonic increasing evolution of both variables, followed by a stabilization.

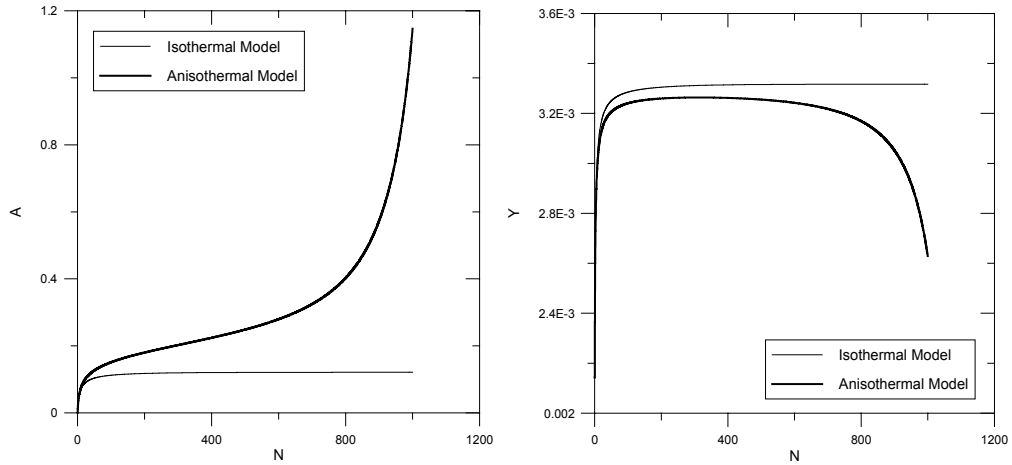

(a) **(b)**

Figure 8: (a) Isotropic hardening evolution; (b) Yield function evolution.

Figure 9 presents a comparison between the phase plane orbits on the last loading cycle for some of the preceding examples. Again, it is possible to observe the differences between the two models. Isothermal model predict orbits that remains the same when an elastic behavior is reached. On the other hand, when the unstable response is present, anisothermal model predict a progressive expansion of the orbits (Figure 9b,c,d). When a stable response is present, both models present the same behavior (Figure 9a).

Conclusions

This contribution reports to a dynamical analysis of an elasto-plastic oscillator where the thermomechanical coupling is considered. A constitutive model with isotropic hardening is presented. Operator split technique is used for the numerical solution. A numerical method is developed using an implicit integration scheme associated with the return mapping algorithm. The proposed return mapping algorithm treats the coupled mechanical and thermal equations simultaneously, which permits the use of relatively large time steps. Some numerical simulations show that the isothermal model, where thermomechanical coupling is not considered, tends to present an elastic stabilized response. On the other hand, the numerical results obtained with anisothermal model may present an unstable behavior to some special values of the parameters.

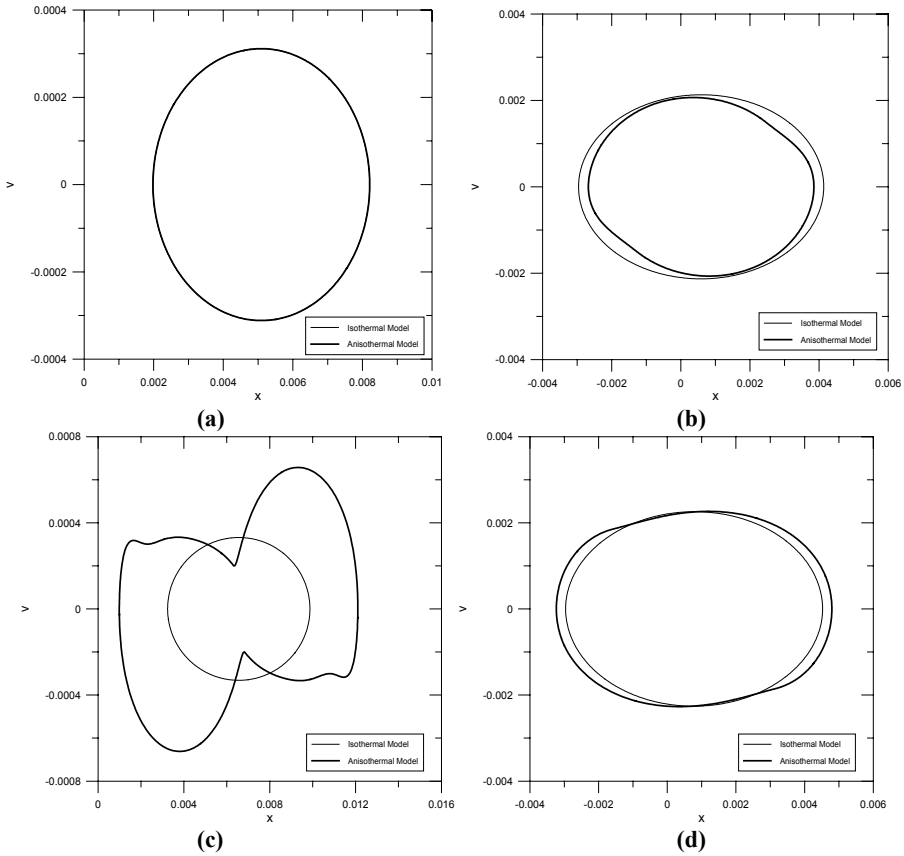

Figure 9: Phase plane orbits predicted by isothermal and anisothermal models.
(a) F_0 = 3.1e-3 and Ω = 0.1 ; (b) F_0 = 3.1e-3 and Ω = 0.6 ;
(c) F_0 = 3.3e-3 and Ω = 0.1 ; (d) F_0 = 3.3e-3 and Ω = 0.6.

References

Chorin, A., Hughes, T.J.R., McCracken, M.F. and Marsden, J.E., 1978, "Product Formulas and Numerical Algorithms", *Commun. Pure Appl. Math.*, 31, pp.205-256.

Lemaitre, J. and Chaboche, J.L., 1990, "*Mechanics of Solids Materials*", Cambridge Univ. Press.

Luenberger, D.G. (1973), "*Introduction to Linear and Nonlinear Programming*", Reading, Addison-Wesley.

Marchuck, G.L., 1975, "*Methods of Numerical Analysis*", Springer-Verlag.

Ortiz, M., Pinsky, P.M. and Taylor, R.L., 1983, "Operator Split Methods for the Numerical Solution of the Elastoplastic Dynamic Problem", *Computer Methods Appl. Mech. Eng.,* **39**, pp.137-157.

Pacheco, P.M.C.L., 1994, "*Analysis of the Thermomechanical Coupling in Elasto-viscoplastic Materials*", Doctoral Thesis, Dept. of Mechanical Engineering, PUC-Rio (in portuguese).

Simo, J.C., 1994, "*Topics on the Numerical Analysis and Simulation of Plasticity*", Handbook of Numerical Analysis.

Simo, J.C. and Miehe, C., 1992, "On the Coupled Thermomechanical Treatment of Necking Problems via Finite Element Methods", *J. of Appl. Methods in Eng.*, 33, pp.869-883.